

Application of eV neutron scattering and eV neutron absorption techniques

S. Ikeda

National Laboratory for High Energy Physics
Oho, Tsukuba-shi, Ibaraki-ken, 305
JAPAN

Intense spallation neutron sources can provide a useful eV neutron flux in the energy range 1-100 eV, which is much more intense than has ever been available from steady state sources, and makes two fruitful techniques possible. One is an eV neutron scattering technique, which allows the impulse approximation limit to be approached. In this limit, the scattering function is simply related to the momentum distribution $n(p)$ of the struck particle (mass M) by [1,2]

$$S(Q, \hbar\omega - R) = \int dp \delta(\hbar\omega - R - \hbar Q \cdot p/M) n(p), \quad (1)$$

where $\hbar Q$ is the momentum transfer and $R = \hbar^2 Q^2 / 2M$ the recoil energy. If $n(p)$ is Gaussian, $S(Q, \hbar\omega - R)$ can be written as

$$S(Q, \hbar\omega - R) = (\sqrt{2\pi}\sigma_R)^{-1} \exp(-(\hbar\omega - R)^2 / 2\sigma_R^2). \quad (2)$$

In this equation, $\sigma_R = \sqrt{2Rk_B T_{\text{eff}}}$ and $k_B T_{\text{eff}} = (2/3) \langle K \rangle$, where $\langle K \rangle$ and T_{eff} are the mean kinetic energy and the effective temperature, respectively. The mean kinetic energy and the effective temperature are related to the density-of-state $f(E)$. Thus,

$$k_B T_{\text{eff}} = (2/3) \langle K \rangle = (1/2) \int_0^{E_D} E f(E) \coth(E/2k_B T) dE. \quad (3)$$

T is the real temperature of a sample and E_D the maximum energy of $f(E)$. If $f(E) \propto E^2$ (Debye model), T_{eff} is given by

$$k_B T_{\text{eff}} = (3/2) \int_0^{k_B \theta_D} E^3 \coth(E/2k_B T) dE / (k_B \theta_D)^3, \quad (4)$$

where θ_D is the Debye temperature. This method has been applied to measure-

ments of the momentum distribution in pyrolytic graphite, superfluid helium and metal hydrides. Some successful results have already been obtained [3,4,5]. In eV neutron scattering, atoms in a solid are considered to be "free atoms". Hence, the overall scattering function, S_{total} , for a mixed system, such as compounds and alloys, should be written as a sum of the scattering functions of atoms A,B,C... :

$$S_{total} = \sum_{i=A,B,C\dots} \sigma_S^{(i)} \cdot N_d^{(i)} \cdot S^{(i)}(Q, \hbar\omega - R_{(i)}), \quad (5)$$

where $R_{(i)}$, $\sigma_S^{(i)}$ and $N_d^{(i)}$ are the recoil energy, neutron scattering cross section and number density. Let's consider a compound composed of two kinds of atoms (A and B ; $M_B > M_A$). If $R_A \gg R_B$, S_{total} has two distinct peaks around $\hbar\omega = R_A$ and $\hbar\omega = R_B$, corresponding to scattering from atoms A and B. This unique nature of eV neutron scattering provides an opportunity for the direct observation of the motion of a specific atom, separated from the others.

Another one is an eV neutron absorption technique. Many heavy atoms, such as *Ta*, *U*, *Sb*, *Ba* and *Ho*, have large neutron resonant absorption in the energy range 1-100 eV, and the cross section of neutron absorption, σ , is also described using the effective temperature in the weak binding approximation, as follows [6]:

$$\sigma = \sigma_0 \xi (2\sqrt{\pi})^{-1} \int dy \exp[-(\xi/2)^2(x-y)^2/(1+y^2)], \quad (6)$$

where $x = 2(E - E_0 - R)/\Gamma_i$, $\xi = \Gamma_i/\Delta$, $R = (m/M)E_0$ and $\Delta = 2\sqrt{Rk_B T_{eff}}$. Here, m is the neutron mass and σ_0 the peak cross section of neutron absorption. The intrinsic line width, Γ_i , is defined as the full width at half-maximum of the resonance. Since a specific atom is identified by the resonance energy, E_0 , one can measure the effective temperature of the specific atom by using the width of the resonance peak, apart from the other atoms in a mixed system. The finite thickness of the absorbing material leads to self-shielding effects, and the probability for neutron absorption is given by [6]

$$P_A(E) = 1 - \exp(-n_d \sigma), \quad (7)$$

where n_d is the number density of the resonant absorbing atoms per unit area perpendicular to the neutron beam.

A schematic layout of an eV neutron scattering spectrometer is shown in Fig.1(a). Pulsed white neutrons produced at t_0 on the moderator are scattered by a sample, and the scattered neutrons of final energy E_f are captured by a resonance foil. The probability of neutron absorption of the resonance foil also can be described by $P_A(E_f)$ in Eq.(7). Promptly after the neutron capture, a γ -cascade is emitted from the resonance foil, which is detected by a scintillator. The energy of the incoming neutrons is determined by the time-of-flight(TOF). In this geometry, the TOF scattering spectrum $I_S(t)$ is given by

$$I_S(t) = \int dX_M dX_S dX_D dE_f dE_i dt_0 P_A(E_f) I(E_i, t_0) \delta(t - t_0 - l_i/v_i - l_f/v_f) \\ \times \sqrt{E_f/E_i} \cdot S(Q, \omega - R), \quad (8)$$

where $l_i = |X_m - X_s|$, $l_f = |X_s - X_D|$, $\cos \theta = (X_M - X_S) \cdot (X_S - X_D) / l_i l_f$ and $(M/m)R = \hbar^2 Q^2 / 2m = E_i + E_f - 2\sqrt{E_i E_f} \cos \theta$. Here, $I(E_i, t_0)$ is the neutron intensity of energy E_i at the emission time t_0 on the moderator. E, v and l are the neutron energy, neutron velocity and flight path length, respectively, and i and f refer to incoming and scattered neutrons. X_M, X_S and X_D represent positions on the moderator, the sample and the detector, respectively. Fig.1(b) shows a schematic layout of the neutron absorption spectrometer. The prompt capture γ -cascade produced in the sample is detected by a scintillator and the energy of the incoming neutrons is determined by TOF. The TOF spectrum of the resonant neutron absorption, $I_A(t)$, is given by

$$I_A(t) = \int dE_f dE_i dt_0 P_A(E_f) I(E_i, t_0) \delta(t - t_0 - l_i/v_i). \quad (9)$$

The discovery of superconductivity in the temperature range 30-100 K for the La-Cu-O system [7] and the Y-Ba-Cu-O system [8,9] is one of the most exciting events in the recent solid state physics. Many attempts to explain such

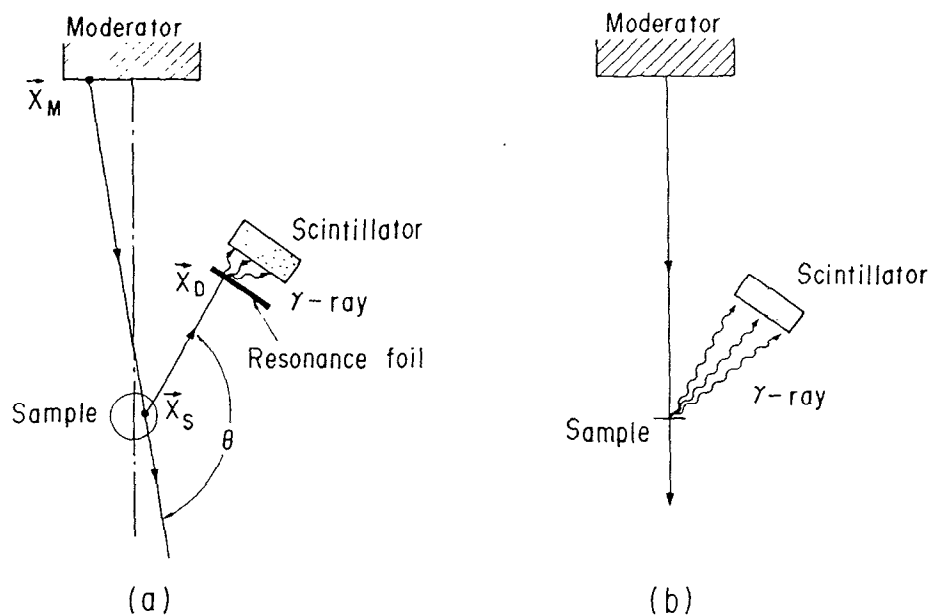


Fig. 1 Layout of an eV neutron scattering spectrometer (a) and a neutron absorption spectrometer (b).

extraordinarily high T_c values have been made with the conventional electron-phonon coupling theory [10,11] as well as with non-phonon mechanisms [12]. The most direct test for such theories is to look for the predicted excitations by using inelastic neutron scattering techniques. Actually, many experiments have been performed using thermal and epithermal neutrons in the energy range $E_i \ll 1$ eV [13,14]. As mentioned above, the eV neutron scattering and eV neutron absorption experiments also can provide new important information for the understanding of the high- T_c mechanism, which has never been obtained by ordinary neutron scattering experiments. For the first time, I applied these methods to the observation of the motions of the specific atoms in La-Cu-O and Y-Ba-Cu-O systems. In this paper, I will report a procedure of the application.

Each powder sample of copper metal, CuO , La_2CuO_4 and $YBa_2Cu_3O_7$, was held in a zirconium cell of 10-mm diameter, 8-cm height and 50- μm thickness, and set at a distance of 8.361 m from the moderator surface. A resonance foil of tantalum (5 cm \times 5 cm) at room temperature was installed at a distance

of 0.15 m from the sample with fixed at an angle of 159 degrees. Scattered neutrons with a final energy of $E_f = 4.28$ eV were detected by a tantalum foil with a scintillator. In these conditions, $Q \sim 90 \text{ \AA}^{-1}$ was realized. Figs.2, 3, 4 and 5 show the neutron scattering TOF spectra of copper metal, CuO , La_2CuO_4 and $YBa_2Cu_3O_7$, in which the background has been subtracted. These TOF spectra were measured at a channel width of $0.5 \mu\text{sec}$. I calculated the single scattering and multiple scattering TOF spectra and plotted them in Figs.2, 3, 4 and 5 as solid and dotted lines. In these figures, the thin solid lines, the dotted lines and the thick solid lines represent the single scattering spectra calculated by Eq.(8), calculated double scattering spectra and the sum of those, respectively. In the case of copper metal, the effective temperature at $T = 300$ K was calculated to be 319 K using the Debye temperature of copper metal, $\theta_D = 343$ K (see Eq.(4)). The TOF spectrum was calculated with $T_{\text{eff}} = 319$ K and compared with the measured data. Good agreement between the calculated spectrum and the measured data was obtained, as shown in Fig.2. This result suggests that the Debye temperature can be well estimated from the effective temperature using Eq.(4). For a mixed system, such as CuO , the TOF spectrum should be calculated using Eqs.(5) and (8). A fit was made to the measured spectrum using the effective temperatures of Cu and O as parameters. A satisfactory fit to the measured spectrum was obtained with $T_{\text{eff}} = 375$ K for Cu and $T_{\text{eff}} = 550$ K for O , as shown in Fig.3. For a more complicated compound, such as La_2CuO_4 , the TOF spectrum can also be calculated by using Eqs.(5) and (8). The total scattering S_{total} in Eq.8 should be written as the sum of three components. A similar fit was made to the measured spectrum of La_2CuO_4 using the effective temperatures of Cu , O and La as parameters. A good fit was obtained with $T_{\text{eff}} = 600$ K for Cu , $T_{\text{eff}} = 550$ K for O and $T_{\text{eff}} = 500$ K for La , as shown in Fig.4.

$YBa_2Cu_3O_7$ is a very complicated system comprising four kinds of atoms. It is, of course, possible to perform a similar fit with many parameters, though a precise determination of the effective temperatures seems to be very difficult. Therefore, I tried, at first, to determine the effective temperatures of Ba and Y

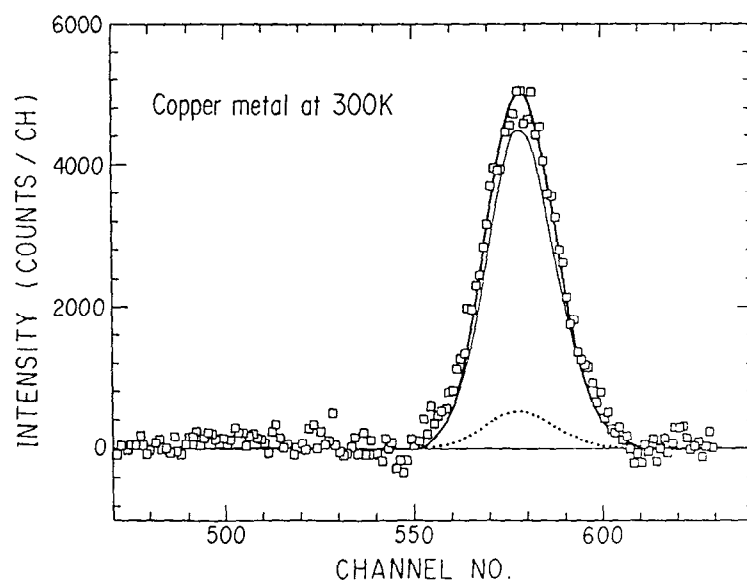


Fig. 2 Neutron scattering spectrum of copper metal at 300 K. The thick solid line is a calculated spectrum with $T_{\text{eff}}=319$ K. The thin solid line and dotted line are calculated single and multiple scattering, respectively.

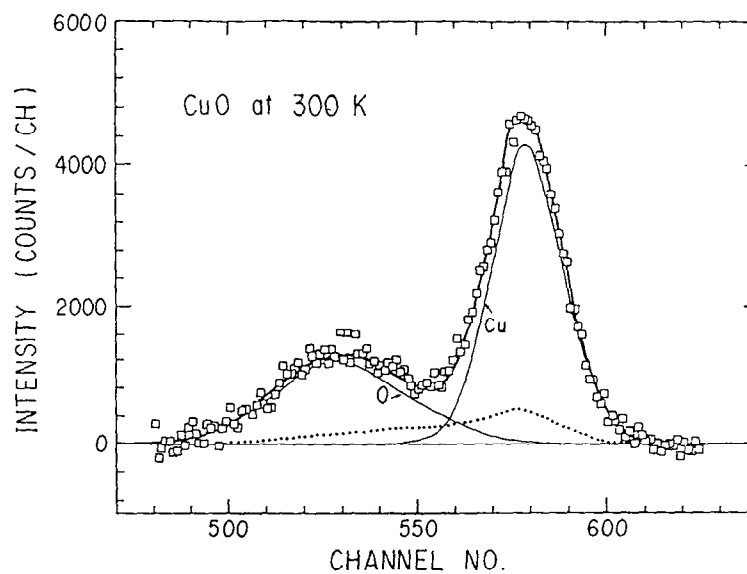


Fig. 3 Neutron scattering spectrum of CuO at 300 K. The thick solid line is a calculated spectrum with $T_{\text{eff}}=375$ K (Cu) and $T_{\text{eff}}=550$ K (O). The thin solid line and the dotted line are calculated single and multiple scattering, respectively.

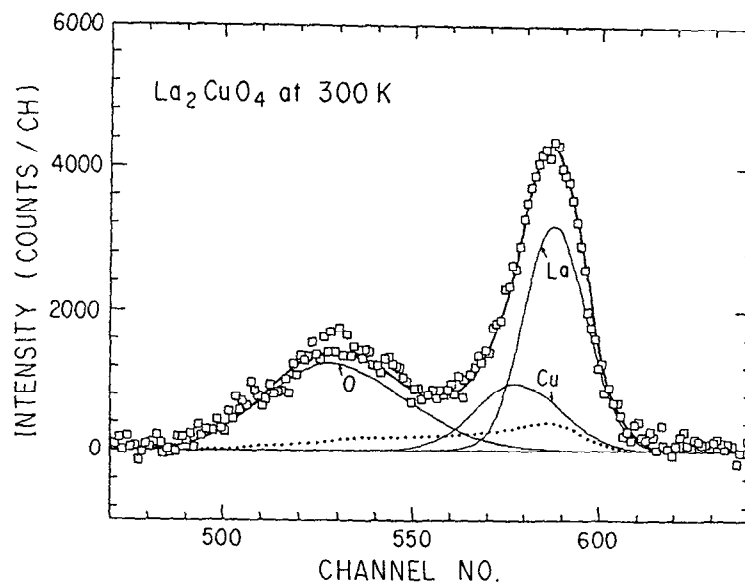


Fig. 4 Neutron scattering spectrum of La_2CuO_4 at 300 K. The thick solid line is a calculated spectrum with $T_{\text{eff}}=600\text{K}$ (Cu), $T_{\text{eff}}=550\text{K}$ (O) and $T_{\text{eff}}=500\text{K}$ (La). The thin solid lines and the dotted line are calculated single and multiple scattering, respectively.

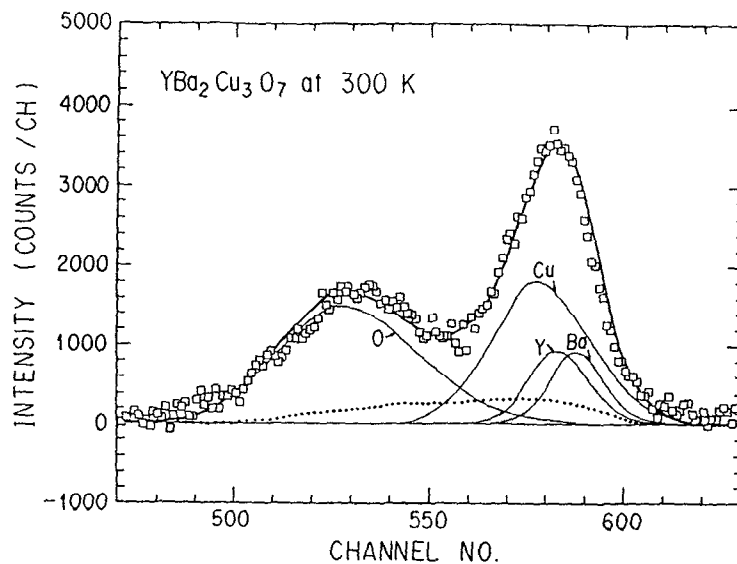


Fig. 5 Neutron scattering spectrum of $\text{YBa}_2\text{Cu}_3\text{O}_7$ at 300 K. The thick solid line is a calculated spectrum with $T_{\text{eff}}=750\text{K}$ (Cu), $T_{\text{eff}}=550\text{K}$ (O), $T_{\text{eff}}=300\text{K}$ (Ba) and $T_{\text{eff}}=300\text{K}$ (Y). The thick solid lines and the dotted line are calculated single and multiple scattering, respectively.

by neutron absorption experiments, and then to fit to the measured data using only two effective temperatures of *Cu* and *O* as parameters. I performed neutron absorption experiments on $HoBa_2Cu_3O_7$ instead of $YBa_2Cu_3O_7$, since ^{165}Ho and ^{135}Ba have very large neutron resonant absorptions at 3.92 eV and 24.4 eV, respectively. However, *Y* has no neutron resonant absorption in the energy range 1-100 eV. $HoBa_2Cu_3O_7$ is isostructural to $YBa_2Cu_3O_7$, and its transition temperature is the same as that of $YBa_2Cu_3O_7$ [15]. Therefore, the effective temperatures of *Ho* and *Ba* in $HoBa_2Cu_3O_7$ is considered to be the same as those of *Y* and *Ba* in $YBa_2Cu_3O_7$. In order to test the neutron absorption spectrometer, neutron absorption experiments were performed on holmium metal foil ($5\text{ cm} \times 5\text{ cm}$, $25\text{ }\mu\text{m}$) at 300 and 20 K. The TOF spectra, $I_A(t)$, was calculated by Eq.(9) and fitted to the measured spectra using the effective temperature of *Ho* as a parameter. Excellent fits to the measured spectra at 300 and 20 K were obtained with $T_{\text{eff}} = 300\text{ K}$ and $T_{\text{eff}} = 80\text{ K}$, respectively. In the calculation of $I_A(t)$, I used $\Gamma_i = 87\text{ meV}$ and $\sigma_0 = 9510\text{ barn}$, which were taken from ref.(16), and $n_d = 7.95 \times 10^{19}\text{ cm}^{-2}$ which was calculated from the foil thickness. These results were consistent with a previous measurement [17].

I prepared a sample of $HoBa_2Cu_3O_7$ ($2\text{ cm} \times 2\text{ cm}$ and 0.2 mm thick) and set it on the sample position. n_d 's of *Ho* and *Ba* in this sample, were $6.5 \times 10^{19}\text{ cm}^{-2}$ and $13 \times 10^{19}\text{ cm}^{-2}$, respectively. Figs.6 and 7 show the TOF neutron absorption spectra of *Ho* and *Ba* in $HoBa_2Cu_3O_7$, which were simultaneously measured at 300 and 20 K. The channel width was $0.125\text{ }\mu\text{sec}$. $I_A(t)$ for *Ho* in $HoBa_2Cu_3O_7$ was calculated with the same values of Γ_i and σ_0 as those used in the calculation for holmium metal. The solid lines in Figs.6(a) and (b) were calculated with $T_{\text{eff}} = 300\text{ K}$ and $T_{\text{eff}} = 80\text{ K}$, respectively. Excellent agreement with the measured spectra was obtained. Note that the effective temperatures of *Ho* in $HoBa_2Cu_3O_7$ are the same as those of holmium metal at both 20 and 300 K. These results indicate that the Debye temperature of *Ho* in $HoBa_2Cu_3O_7$ is the same as that of holmium metal. $I_A(t)$ for *Ba* in $HoBa_2Cu_3O_7$ was also calculated using $\Gamma_i = 124\text{ meV}$ and $\sigma_0 = 4680\text{ barn}$, taken from ref.(16). Since the Debye temperature of barium metal is 116 K,

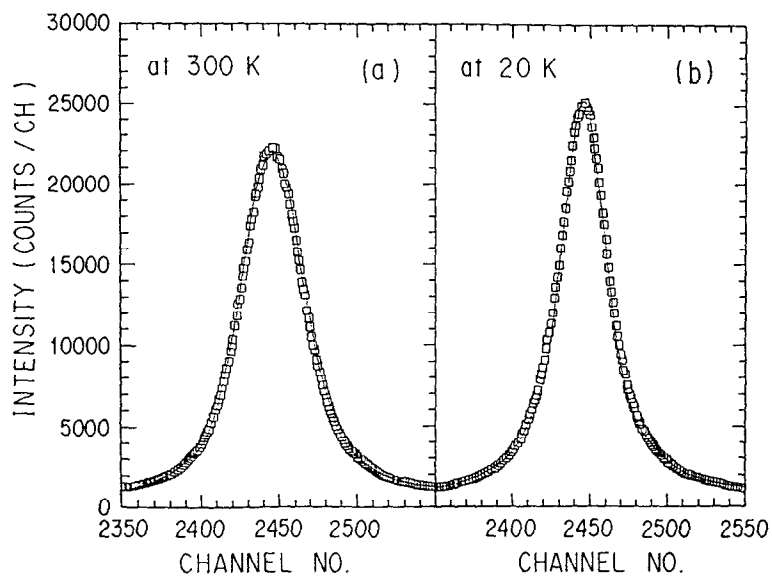


Fig. 6 Neutron absorption spectra of Ho in $\text{HoBa}_2\text{Cu}_3\text{O}_7$ at 300 K and 20 K. The solid lines are the calculated spectra with $T_{\text{eff}}=300$ K (a) and $T_{\text{eff}}=80$ K (b), respectively.

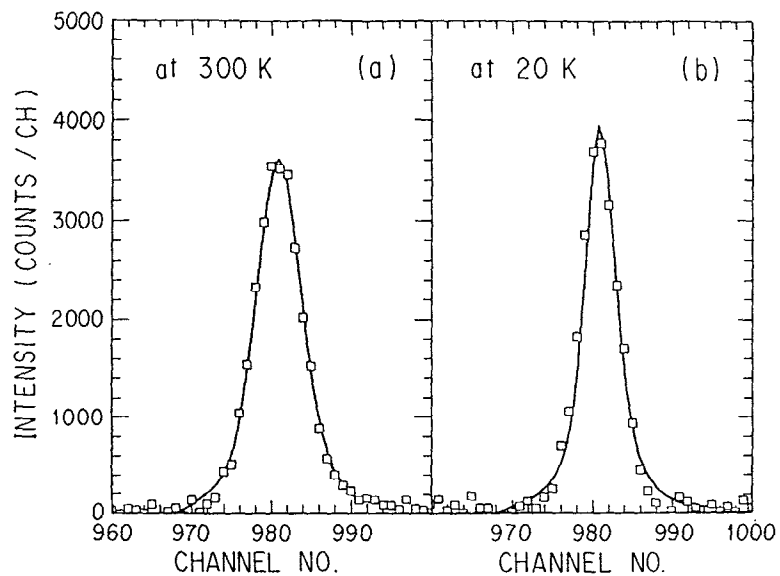


Fig. 7 Neutron absorption spectra of Ba in $\text{HoBa}_2\text{Cu}_3\text{O}_7$ at 300 K and 20 K. The solid lines are calculated spectra with $T_{\text{eff}}=300$ K (a) and $T_{\text{eff}}=45$ K (b), respectively.

the effective temperatures of barium metal at $T = 20$ K and $T = 300$ K were calculated to be 45 and 300 K, respectively. The solid lines in Figs.7(a) and (b) were calculated with $T_{\text{eff}} = 300$ K and $T_{\text{eff}} = 45$ K, respectively. Good agreement with the measured spectra was obtained. These results also indicate that the Debye temperature of *Ba* in $HoBa_2Cu_3O_7$ is the same as that of barium metal. From these results, the effective temperatures of *Y* and *Ba* in $YBa_2Cu_3O_7$ at $T = 300$ K were assumed to be $T_{\text{eff}} = 300$ K. Then, the effective temperatures of *Y* and *Ba* were fixed and a fit was made to the neutron scattering spectrum of $YBa_2Cu_3O_7$ using the effective temperatures of *Cu* and *O* as parameters. A satisfactory fit to the measured spectrum was obtained with $T_{\text{eff}} = 750$ K for *Cu* and $T_{\text{eff}} = 550$ K for *O*, as shown in Fig.5.

Table I shows the effective temperatures of *O* and *Cu* in copper metal, CuO , La_2CuO_4 and $YBa_2Cu_3O_7$, obtained by the present experiments. Note that the effective temperature of *O* is 550 K in CuO , La_2CuO_4 and $YBa_2Cu_3O_7$. This value is almost the same as the effective temperature of *O* in H_2O at $T = 300$ K, $T_{\text{eff}} = 500$ K [5]. My results may suggest that the effective temperature of *O* is almost independent of the structure and the bonding atom. The most interesting result in my experiments is that the effective temperatures of *Cu* in La_2CuO_4 and $YBa_2Cu_3O_7$ are much larger than those of CuO and copper metal, and that the effective temperature of *Cu* in $YBa_2Cu_3O_7$ is larger than that in La_2CuO_4 . The neutron absorption spectra of *Ta* in TaC and Ta_2O_5 were measured in order to determine the effective temperatures of *Ta*. The results show that the effective temperatures of *Ta* are almost the same as that of tantalum metal in a wide temperature range of 40 - 300 K [17]. Generally, the effective temperature of a heavy atom in a compound with light atoms is considered to be the same as that of the pure heavy atom's metal, independently of the bonding atoms. My results for *Cu* in La_2CuO_4 and $YBa_2Cu_3O_7$ are opposed to 'the sound consideration'. This suggests that the *Cu* vibration is abnormal in La_2CuO_4 and $YBa_2Cu_3O_7$. It might be interesting to calculate the Debye temperature by Eq.(4) in order to make a rough estimate of the density-of-state. The dashed line in Fig.8 shows the relation between the Debye

temperature and the effective temperature at $T = 300$ K. By this relation, the Debye temperature of O was determined to be about 1400 K, and the Debye temperatures of Cu in La_2CuO_4 and $YBa_2Cu_3O_7$ were determined to be about 1500 and 2000 K, respectively. This indicates that the O vibration spectrum extends to 120 meV in CuO , La_2CuO_4 and $YBa_2Cu_3O_7$, and that Cu vibrations in La_2CuO_4 and $YBa_2Cu_3O_7$ may extend to 130 and 170 meV, respectively.

	O $T_{eff}(K) / \theta_D(K)$	Cu $T_{eff}(K) / \theta_D(K)$
Copper metal	————	319 / 343
CuO	550 / 1400	375 / 700
La_2CuO_4	550 / 1400	600 / 1500
$YBa_2Cu_3O_7$	550 / 1400	750 / 2000

Table I Effective temperatures and the Debye temperatures of O and Cu.

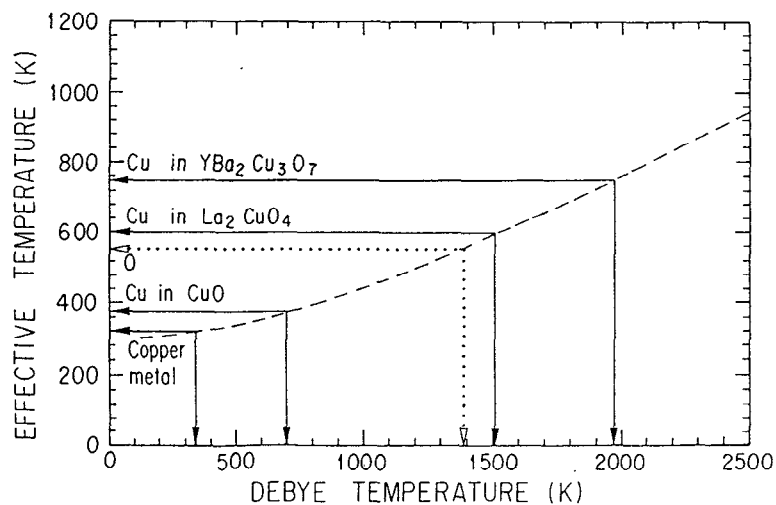


Fig. 8 Relation between the effective temperature and the Debye temperature at 300 K.

References

1. P.C. Hohenberg and P.M. Platzman, *Phys. Rev.* 152(1966) 196.
2. M.S. Nelkin and D.E. Parks, *Phys. Rev.* 119(1960) 1060.
3. H. Rauh and N. Watanabe, *Phys. Lett. A* 100 (1984) 244.
4. S. Ikeda and N. Watanabe, *Phys. Lett. A* 121 (1987) 34.
5. A.D. Taylor, *Proceedings of the 1984 Workshop on High-Energy Excitations in Condensed Matter* (Feb., 1984, Los Alamos) p.512.
6. W.E. Lamb, *Phys. Rev.* 55 (1939) 190.
7. J.G. Bednorz and K.A. Muller, *Z Phys. B* 64 (1986) 18.
8. M.K. Wu, J.R. Ashburn, C.J. Torng and P.H. Hor, R.L. Meng, L. Gao, Z.J. Huang, Y.Q. Wang and C.W. Chu, *Phys. Rev. Lett.* 58 (1987) 405.
9. C. Politis, J. Greek, M. Dietrich, B. Obst and H.L. Luo, *Z. Phys. B* 66 (1987) 279.
10. L.F. Matthesis, *Phys. Rev. Lett.* 58 (1987) 1028.
11. W. Weber, *Phys. Rev. Lett.* 58 (1987) 1371.
12. P.W. Anderson, *Science* 235 (1987) 1196.
13. B. Renker, F. Gompf, N. Nucker, D. Ewert, W. Reichardt and H. Rietschel, *Z. Phys. B* 67 (1987) 15.
14. B. Renker, F. Gompf, E. Gering, G. Roth, D. Ewert, W. Reichardt and H. Rietschel, *Physica C* 153-155 (1988) 272.
15. H. Asano, K. Takita, T. Ishigaki, H. Akinaga, H. Katoh, K. Masuda, F. Izumi and N. Watanabe, *Jpn. J. Appl. Phys.* 26 (1987) L1341.
16. *Neutron cross sections*, 3rd Ed., BNL 325 (1973).
17. H. Rauh and N. Watanabe, *Nucl. Instrum. Methods* 222 (1983) 507.